PRASHANT KUMAR NAYAK
A K DASH
and
PANKAJ DEWANGAN

Investigating the effects of rainfall and groundwater on coal mine waste dump stability: a case study

Sudden inrush of rainwater in the waste dump as well as the saturation of the dump material in case it is constructed near the source of water, increases the risk of dump failures due to water infiltration through the dump. A number of dump failures have been reported in the past during monsoon season. Understanding the hydrogeology of the project area and prospective sites should be required to be considered while designing and constructing the dumps. High groundwater levels and pore pressures in the dump foundation adversely affect the static dump stability. Construction of waste dump changes the natural ground levels and flow regime. Water induced failure like ponding of surface should be avoided, particularly adjacent to dump crests by drainage ponding. In this present study, the rainfall-induced waste dump profile of the Srirampur opencast project is addressed by understanding its climatic and hydrogeological conditions. An infiltration analysis of single event rainfall conditions was performed with a focus on cumulative rainfall calculations. Instability calculations need consideration for the seepage force which is an internal force when the soil grains alone and soil skeleton plus the water are considered for the free body. For this purpose, under the steady-state time-dependent flow, an analysis on the influence of single event rainfall was built from the rainfall data to know the parameters for infiltration and seepage conditions. Stability calculations were performed in FLAC^{2D} for any uplift force exertion on the bottom of the coal waste dump in the operating mining conditions.

Keywords: *Waste dump, dump stability, rainfall, groundwater, infiltration, saturation, pore pressure.*

1.0 Introduction

High and steep slopes with shallow groundwater table are more vulnerable in case of sudden and heavy rainfall (Ng and Shi, 1998; Rahardjo et al., 2007). One of the severe waste dump failures that occurred in the coal mine waste tip in Wales in 1966 was attributed to a build-up of pore pressure in the waste material due to heavy rains and natural springs in the foundation which triggered a liquefaction-type failure. Runout from this failure inundated a primary school and residential section in the town of Aberfan, killing 116 children and 28 adults (Hawley and Cunning, 2017). The slope geometry and the initial water table determine the initial FoS, and the actual failure conditions are much affected by rainfall characteristics and properties of the soils in the slope (Rahardjo et al., 2007; Nayak et al., 2019; Dash 2019; Nayak et al., 2021). The infiltration of rainfall into waste dump results in the rise of the groundwater level, a decrease in matric suction and a similar decrease of shear strength of dump material. These, in turn, may trigger slides, mudslides and slope failures of the dumps (Koner and Chakravarty, 2016). Infiltration plays a significant role in the instability of slopes under rainfall conditions. The effect of seepage on slope stability shall be done by calculating the factor of safety (FoS) subject to seepage parallel to the slope surface by assuming saturated steady-state flow up to a particular depth (Collins and Znidarcic, 2004). Hence, the development of seepage forces will depend on the built by the pore water pressure. In this paper, infiltration modelling was performed to contribute to the standard infiltration curve calculations. Steady-state flow methods were performed in a two-dimensional finite-difference solution to acknowledge the waste dump instability determined from the field conditions with the help of numerical analyses.

2.0 Study area

Srirampur opencast project-II block is in the southern part of the Somagudem–Indaram coal-belt between Srirampur-1 Incline and Indaramkhani-1 Incline in the South Godavari valley coalfield. This block is covering an area of 5.33 km^2. The area is covered in Survey of India Toposheet No.56N/5, 56 N/6, 56 N/9 and 56 N/10 and is bounded between the North latitude 18^{o}49$'$04$''$ and 18^{o}51$'$12$''$ and East longitude 79^{o}29$'$17$''$ and 79^{o}32$'$02$''$ (Fig.1). The block is falling in the Mancherial Mandal of Adilabad district in Andhra Pradesh. The OCP forms a part of the Bellampalli region of the Singareni Collieries Company Limited (SCCL). The block area is a plain terrain, gently sloping towards the south. The topographic

Blind peer reviews carried out

Mr. Prashant Kumar Nayak, Research Scholar, Dr. A K Dash, Assistant Professor, and Prof. Pankaj Dewangan, Associate, Department of Mining Engineering, National Institute of Technology, Raipur, India

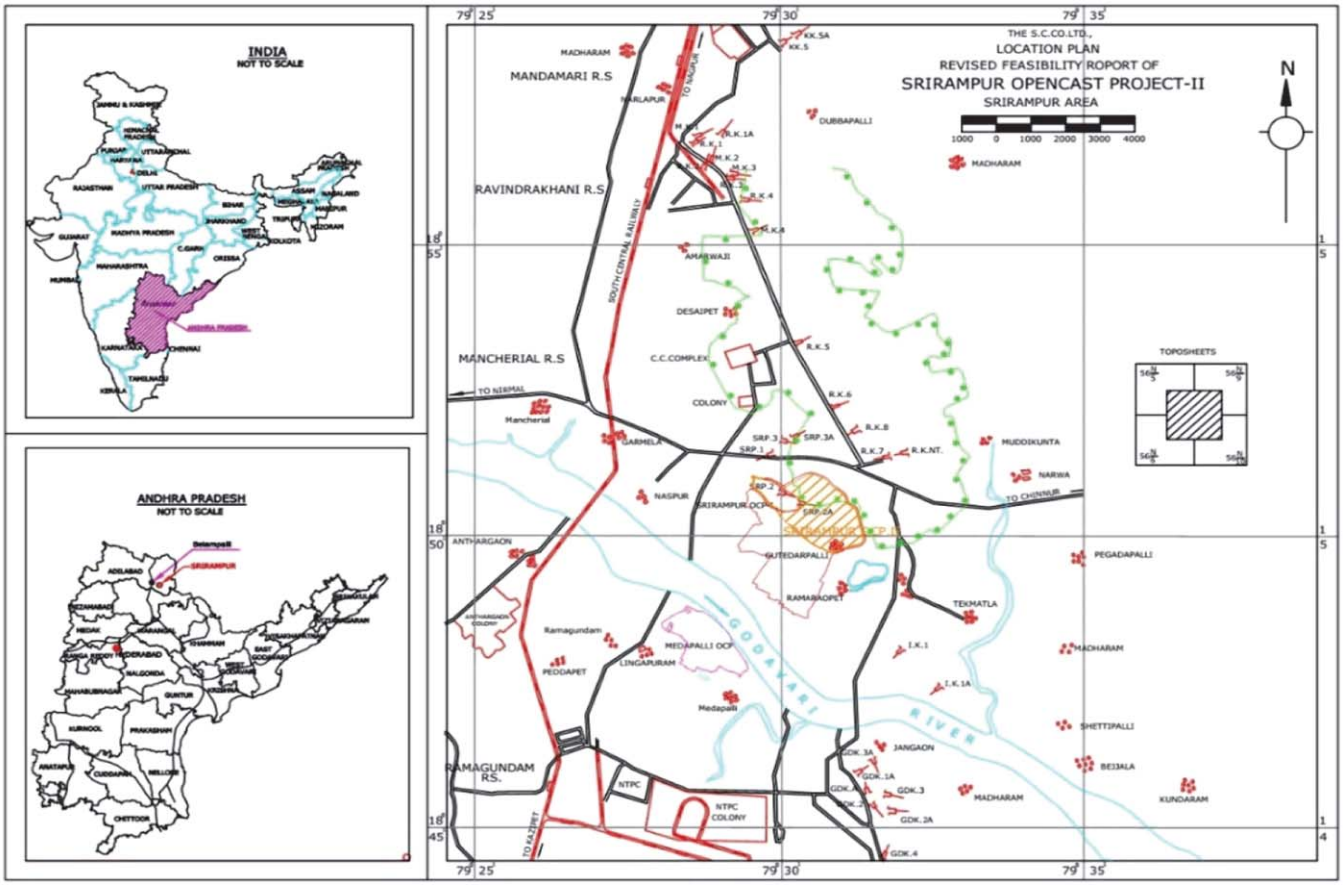

Fig.1: The geographical location of Srirampur OCP-II project

elevation varies from 142.76m to 164.03m above Mean Sea Level (MSL). The lithological details of the block are presented in Table 1.

3.0 Field study and geotechnical assessment

The design of the mine waste dump must incorporate geotechnical failure analysis. Before the construction of large waste dumps foundation analysis is a prerequisite to ensure basal stability. The effects of local groundwater conditions and other geo-hydrologic factors are of utmost consideration in the sitting and designing of the waste dump (Bhattacharya, 2009). The geometrical, constructional and other details of the mine waste are collected, some are given in Table 2. The physico-mechanical properties of the overburden strata are presented in Table 3. The overburden rocks mostly comprised sandstone having cohesion between 32-55 kg/cm^2, internal friction angle of 30^o-42^o for intact rock, and the values are much less for the residual rocks.

4.0 Rainfall infiltration and the effect of pore water pressure

The review of rainfall data shows that the rainy season in the area is active from June and lasts until October, and peak rain is expected during July. The annual intensity and duration of the rainfalls during the selected year are shown in Fig.2.

TABLE 1: LITHOLOGICAL CHARACTERISTICS OF OB OF SRIRAMPUR OCP-II

	Strata	Lithology	Thickness(m)
1	Above I seam	Medium to coarse grain grey sandstones	45-75
2	Parting between I and II seam	Medium grained grey sandstones	10-36
3	Parting between II and III-B seam	Fine-grained to Medium grained grey sandstones	25-50
4	Parting between III-B and III-A seam	Fine-grained to Medium grained white sandstones	6-19
5	Parting between III-A and III seam	Fine-grained white sandstones	9-35

The total rainfall amounts that were measured during a single storm event are given in Table 4. Using the data, the rainfall amounts as the percentage of the total rainfall and the plot of the dimensionless total rainfall curve is obtained. The rainfall height (R) is divided by the final cumulative rainfall amount (R/314) and the storm rainfall duration by 240 (T/240) to get rainfall and time percentages. Hyetograph is plotted to shows the change of rainfall intensity with time during the storm as shown in Fig.3. The change of rainfall intensity $I=\Delta R/\Delta T$ with time is given in Table 6 using the data in Table 5. The start time of rainfall is taken as zero and the

TABLE 2: DETAILS OF OVERBURDEN WASTE DUMP

Features	Study site
Coalfield	Godavari valley
Mining area	Southern part of Somagudem-Indaram coal-belt
Mining method	
Present	Opencast
Type of dump	External
Dumping method	Shovel-dumper (combination)
Dump height	30-90m
External dump	
Overall dump slope	20.74°
Dump slope angle	37.5°

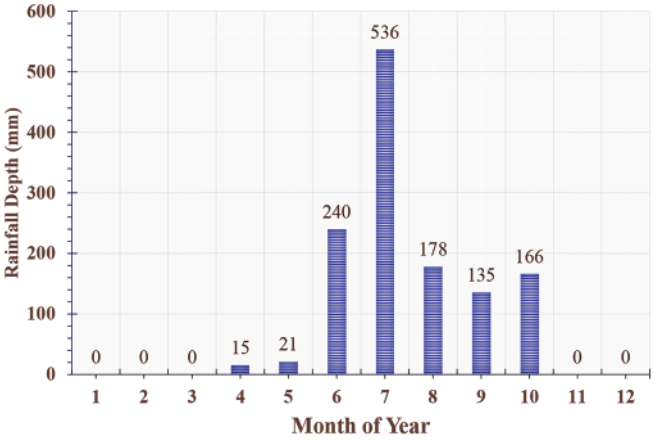

Fig.2: Daily rainfall

Fig.3: Hyetograph

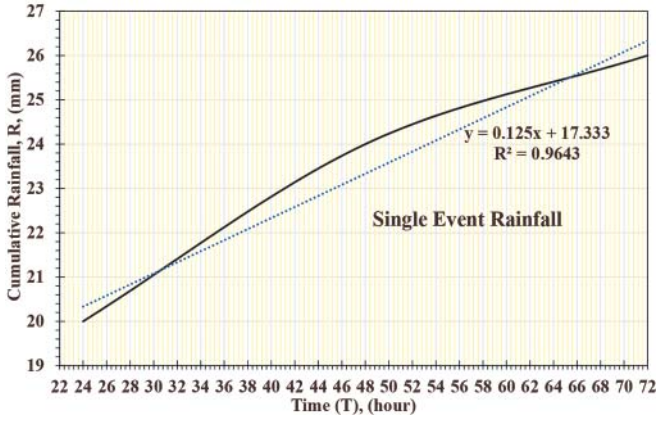

Fig.4: Rainfall-time data

changes in R versus T are rearranged as shown in Table 6 (Sen, 2015).

The cumulative rainfall amounts for the rainfall event for 72 hours duration was interpreted to understand the given rainfall data. The slope of the graph at any point indicates the rainfall intensity. Fig.4 shows the rainfall condition with a high slope at the beginning, which reduces as time increases and at the end; it becomes horizontal, which means the end of a storm event. The change of infiltration capacity by time is calculated and shown in Table 7. The cumulative rainfall curve is shown in Fig.5 and the standard infiltration curve for the event rainfall of 72 hours is shown in Fig.6.

If f_t=the rate of infiltration (mm/hr) and t hours of precipitation occur at rate r (mm/h), f_i = the infiltration rate at t=0 and f_f = the limiting rate of infiltration after a long time, the infiltration curve by (Horton, 1940) is given by $f(t)=f_f+(f_i-f_f)e^{-kt}$ considering f_t=infiltration capacity at instant t after the rainfall started; f_i = initial infiltration capacity=8.3 mm/hr; f_f = final infiltration capacity = 0.3 mm/hr; and k = Infiltration coefficient, we get, $\ln[f_t-f_f] = \ln[f_i-f_f]-k_t$ taking the logarithm of both sides. The results of $\ln[f_t-f_f]$ versus t on semi-logarithmic paper appear to be straight-line. The slope of the straight-line k=0.26 which comes under the high category. For the soil of external dump, the Horton

TABLE 3: PHYSICO-MECHANICAL PROPERTIES OF THE OVERBURDEN ROCK OF SRIRAMPUR OCP-II

	Strata	Dry density (gm/cm^3)	Compressive strength (MPa)	Cohesion (Kg/cm^2)	Angle of friction (°)
1	Medium to coarse-grained grey sandstones	1.91-2.13	7.82	32 - 48	30
2	Medium grained grey sandstones	2.12	17.9	38 - 55	40
3	Fine-grained grey sandstones	2.03	18.0	55	36
4	Coarse-grained white stones	1.91-2.03	10.98	45	35.5
5	Medium grained white stones	2.12	14.8	38	38
6	Fine-grained white stones	2.17	23.48	37	42

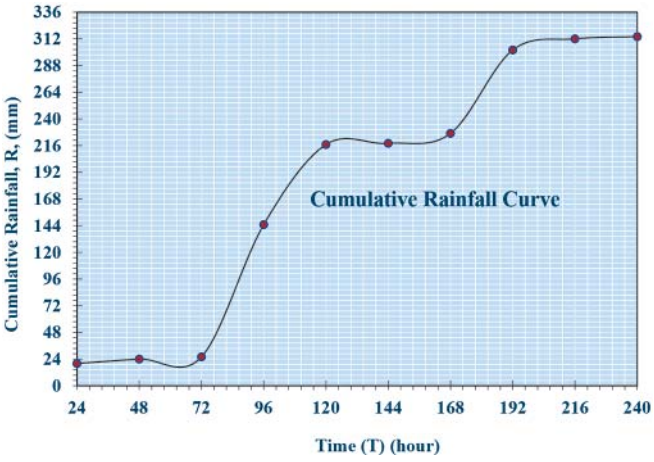

Fig.5: Cumulative rainfall

TABLE 4: PERCENTAGES OF RAINFALL AND TIME

T (hr.)	CR (mm)	T/240	CR/314
24	20	0.10	0.064
48	24	0.20	0.076
72	26	0.30	0.083
96	145	0.40	0.462
120	217	0.50	0.691
144	218	0.60	0.694
168	227	0.70	0.723
192	302	0.80	0.962
216	312	0.90	0.994
240	314	1.00	1.000

TABLE 5: STORM RAINFALL DATA RECORD

Time (hr.)	Cumulative rainfall (mm)	Time (hr.)	Cumulative rainfall (mm)
24	20	144	218
48	24	168	227
72	26	192	302
96	145	216	312
120	217	240	314

TABLE 6: RAINFALL INTENSITY

T	ΔT	R	CR	ΔR	I=ΔR/ΔT
24	-	-	-	-	-
48	24	20	20	4	0.17
72	24	4	24	2	0.08
96	24	2	26	119	4.96
120	24	119	145	52	2.17
144	24	72	217	72	3.00
168	24	1	218	8	0.33
192	24	9	227	75	3.13
216	24	75	302	10	0.42
240	24	10	312	2	0.08

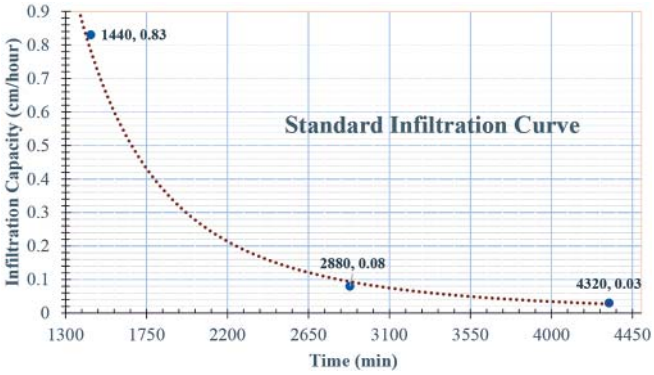

Fig.6: Standard Infiltration curve

TABLE 7: INFILTRATION CAPACITY CHANGES

Time (min)	ΔT (hour)	Added water height (cm)	ΔI	Standard infiltration capacity f=ΔF/ΔT (cm/hour)
0	-	0	-	-
1440	24	2.00	20	0.83
2880	24	0.40	4	0.08
4320	24	0.20	2	0.03

equation f_t=0.03+(0.83–0.03)$e^{-0.26t}$ = 0.03+0.80$e^{-0.26t}$. This indicates that at t=0, f_t=f_0, and at $t = \infty$, $f_t = f_f$, and the value of k is deciding criteria for quantifying that how rapidly $f(t)$ approaches f_f. This equation is an empirical expression that fits the shape of the infiltration curve.

The infiltration in coal mine waste dump can take place by rain infiltration and ponding infiltration where water enters waste dump through its surface when the dump is fully or partially covered by a layer of water. The infiltration rate depends upon soil texture, degree of compaction, and ambient moisture content. Flatter topography would facilitate infiltration, whereas steeper topography would favour runoff. For any given soil under ponded conditions, infiltration rates gradually decrease until they level off at an equilibrium infiltration capacity (Hudak, 2005). The results show that any (rainfall intensity × time) less than the curve would have infiltrated. Any rainfall at an intensity less than the measured limiting rate (f_f) will infiltrate have the potential to enter the waste dump (Blight, 2010).

Based on the intensity of the antecedent water condition of the near-surface materials a proportion will infiltrate into the near-surface layer. The infiltrating water increases the water volume stored in the near-surface layer. For ponding infiltration, the difference between initial soil-water content and the saturation soil-water content determines the infiltration rate. Below the water table, the soil moisture content is constant even though the pressure increases with depth. Above the water table, the water content is a function of the pressure. The pressure becomes more the negative moisture content decreases. By plotting the moisture content against the negative pressure, we get a curve known as the

"moisture characteristic" curve. Each soil is defined by a unique moisture characteristic curve. Therefore, for the infiltration rate, the soil-water content and soil-water matric potential profiles are important since they depend on soil properties (Novak and Hlavacikova, 2019).

As suggested by (Kisch, 1959), under steady-state conditions, the gradient of pore water pressure can be expressed as $\frac{du_w}{dz} = \gamma_w[(\frac{q}{k}) - 1]$. In hydrostatic conditions, there is no ground flux, and the gradient of the pore water pressure head is -1. The pore water pressure profile after 7 days' antecedent rainfall is shown in Fig.7. The study result shows that the higher is the difference between initial soil-water content and soil-water content corresponding to the rain, the higher is the difference in soil-water matric potentials between both soil-water contents and the higher the infiltration rate. Thus, the magnitude of the ground surface flux (q) when reaches the coefficient of permeability of the unsaturated soil (k), for the value of matrix suction, the pressure gradient is zero.

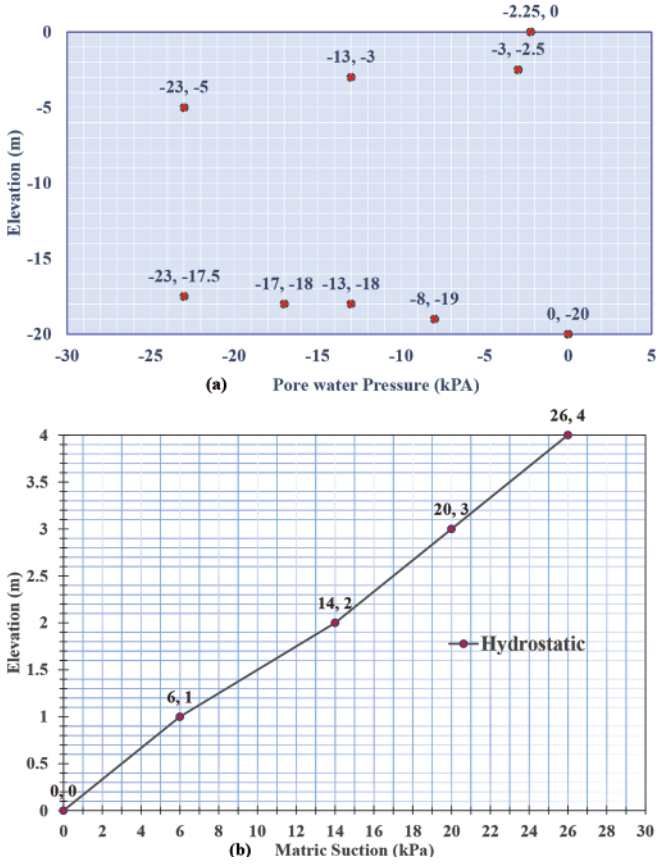

Fig.7: Suction envelope after 7 days' antecedent rainfall

5.0 Dump stability analysis by the FLAC^{2D}

Slope angle and height of dump were observed at 37.5° and 30m are evaluated for overburden dump height of 90m and the base length of 237m. A numerical modelling study was carried out by the finite difference method (FDM). A two-dimensional FDM package FLAC^{2D} (Fast Lagrangian Analysis of Continua) version 7.0 (Itasca, 2011) was utilised for the analysis. Mohr-Coulomb plasticity constitutive model was used to represent the behaviour of dump materials. This means that the soil responds as a linear elastic material until the shear strength is reached such that the use of a constitutive model for the soil that includes plasticity. The boundary conditions were applied as roller boundary along the rear side of the dump and fixed boundary along the base. The flowchart of the methodology adopted for the study as suggested by (Chaulya and Prasad, 2016) is illustrated in Fig.8.

Fig.9 shows the limiting surface created under drained conditions. Numerical analysis shows the FoS of 1.75; indicates that the dump slope under the weight due to the driving forces is stable. The driving forces have not overcome the resisting forces due to soil shear strength and sliding down the dump slope will not occur. The result shows that the dump slope under the drained condition is acutely stable in terms of operating conditions and the probability of failure of the dump is very less than <1% (Hawley and Cunning, 2017).

6.0 Hydrological conditions

The groundwater monitoring wells are surveyed to determine their *x-y* coordinates and elevation. A surveyed reference mark is notched into the top of the well casing; this reference point is used for depth-to-water measurements. Its height is determined within 3mm with mean sea level. To measure the hydraulic head in the monitoring well, the measured water elevation is assigned to the point at the middle of the well's screened interval. In effect, the hydraulic head measurement is averaged across the segment of the well that is open to the aquifer. The hydraulic gradient between two points in an aquifer is the difference of the hydraulic head divided by the distance between the points. In map view or cross-section, data gathered from the three piezometers wells were used to establish the steepest hydraulic gradient, or local direction of groundwater flow (Hudak, 2005). The schematic presentation of key elements for determining the hydraulic head and the hydraulic gradient in an unconfined aquifer as suggested by (Kresic, 2007) is illustrated in Fig.10. Permeability (k) is the measure of the material's capacity to transmit water from one place to another. The travel distance of the tracer concerning time between two wells is $V_a = \frac{r}{t} = \frac{50}{3}$ (m/hr). Seepage velocity is the product of permeability and hydraulic gradient given by $v = k \times i = k \times \frac{h}{L} = k \times \frac{0.16}{50} = \frac{2k}{625}$. The seepage velocity of tracer moves through a permeable material given by $V_a = \frac{r}{n}$ (m/hr). Since the seepage velocity of tracer through the aquifer $V_a = \frac{50}{3}$ m/hr, hence $k = V_a \times V \times n = \frac{50}{3} \times 30 \times 0.25 = 125 \frac{m}{day}$. Therefore, the seepage velocity $(V) = \frac{2k}{625} = \frac{2 \times 125}{625} = \frac{250}{625} = 0.40 \frac{m}{day}$ (Rao, 2017).

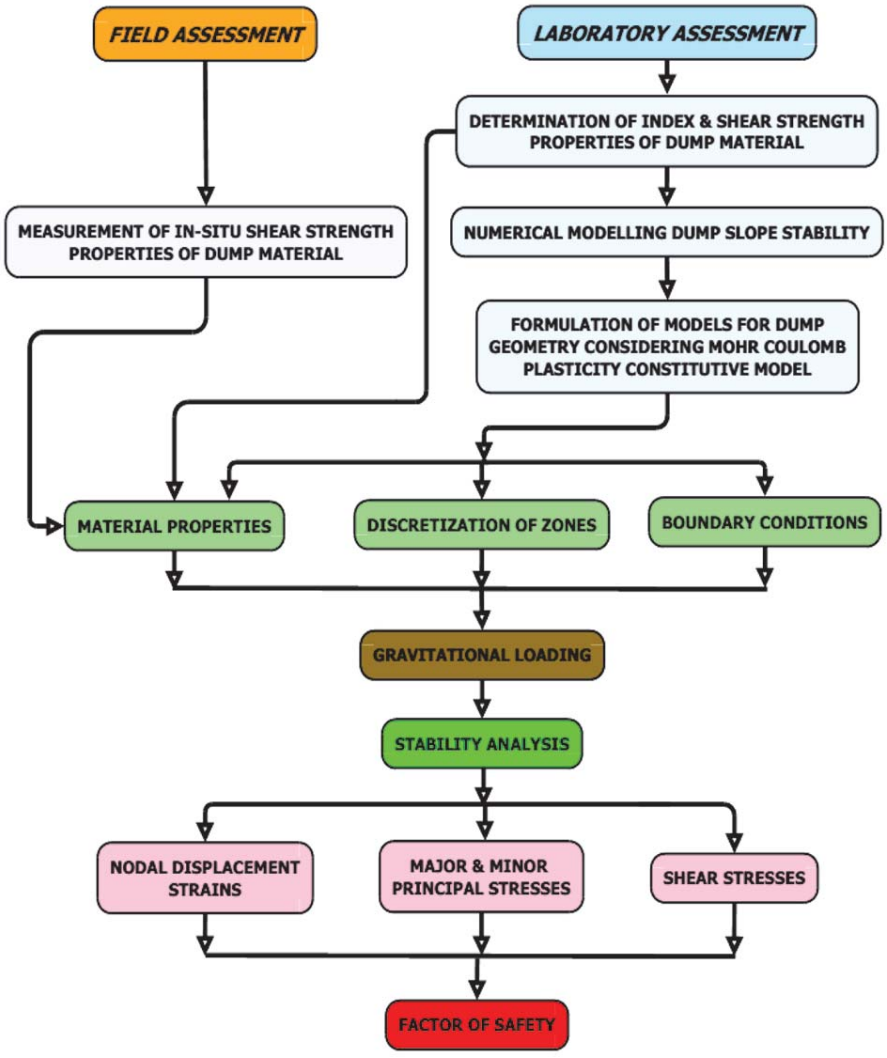

Fig.8: Flowchart of the methodology (Chaulya and Prasad, 2016)

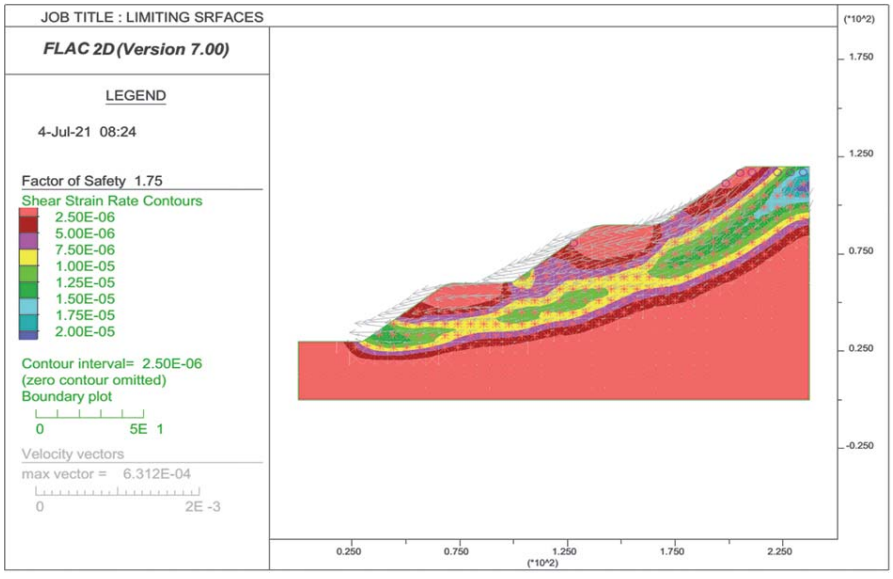

Fig.9: Model showing limiting surface plot and FoS under drained conditions

7.0 Dump stability under steady-state flow

The following assumptions are made for calculations: The soil is uniform with the same permeability in all directions; the soil is saturated with water and the water is in compression; the water is incompressible; Darcy's law governs the water flow through the soil; the flow is in two directions only (x and z, but no flow in the y-direction), and the flow is independent of time: steady-state flow. Fig.11 shows the two free-body diagram options. In the present case study, the free body is the soil particles plus the water, where W = the total weight including the solids and the water; Z_R and Z_L = the total forces; and N' = the effective normal force, U = the uplift force, and T = the shear force, the seepage force is an internal force and is not included in slope stability calculations. However, if the free body is the soil particles alone, W_{subm} = the total weight minus the buoyancy force, $Z_R{}'$ and $Z_L{}'$ = the effective components, N' = the effective normal force and T = the shear force, and the seepage force (E_{seep}) is included in slope stability analysis (Briaud, 2013).

Here four points: (0, 28.50), (130, 28.66), (180, 28.92), and (237, 29.50) defines the location of the water table level and introduces groundwater pressures into the model steady-state flow analysis. The boundary conditions associated are (1) $h(x, y, o) = 0$ for initially dry soil; (2) $h(x, y, t) = f(t)$ on the upstream face; (3) $\frac{\partial h}{\partial y} = 0$ at the impervious base; and (4) $h(x, y, t)$ = the elevation head at free surface (Desai and Zaman, 2014). Considering Δu representing the specified increase in pore pressure at a point x, y (in 2-D), the body force applied to the soil skeleton is the gradient vector that considers a 1.5m rise in the water table in fine-grained grey sandstones. The body force vector is zero everywhere except in the 1.5m high flooded zone. This body force acts upwards (positive in the y-direction) and will cause a heave of the soil surface if this is free,

TABLE 8: MATERIAL PROPERTIES UNDER DRAINED CONDITIONS IN FLAC^{2D}

Material property	Value
Dry Density, γ (kg/m^3)	2100
Internal angle of friction, ϕ (°)	30
Cohesion, c (kPa)	55

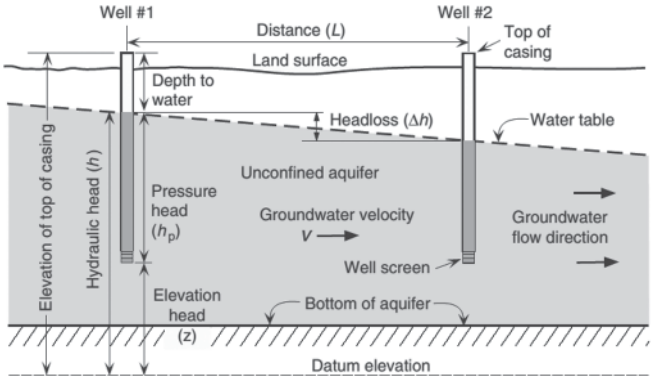

Fig.10: Schematic presentation of key elements for determining the hydraulic head and the hydraulic gradient in an unconfined aquifer (Kresic, 2007)

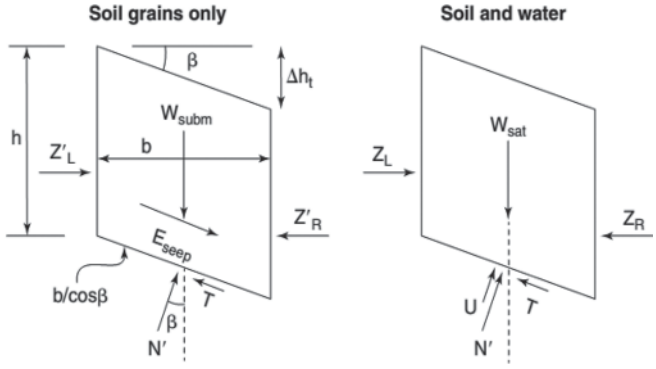

Fig.11: Soil skeleton and seepage force approach (Briaud, 2013)

besides, the weight of water added to the voids are added as downwards (negative) body force (Naylor and Pande, 1981).

Fig.12 shows the FoS value of 1.57 for the performed stability analyses. The maximum shear strain contours are located on the toe of the slope. The concentration of higher shear strain rate is accumulated on the toe of the dump profile. The stresses developed are distributed all along the critical slip surface of the slope mass. The steady-state flow analysis results show that the water stress (pore water pressure) at any point on the bottom of the facility can significantly contribute to the uplift force exertion for the sudden increase and rise of the groundwater table. Therefore, in practice, the placement of coarse durable materials at the base and toe of the waste dump may lower the dump pore pressure and can provide additional internal hydrologic stability. Also, the designed waste dump should provide for controlled water flow to minimizes erosion and enhancing structural stability (Bhattacharya, 2009). FoS value of 1.57 from the stability calculations quantifies a good safety measure as per DGMS (Tech.) Circular No .03 of 2020 Dated 16.02.2020, issued guidelines for Scientific study under regulation 106 of the CMR-2017, which mandates that the minimum factor of safety for a pit, bench and dump slope shall in any case not be less than 1.50 for permanent or long-standing slopes and 1.30 for all others cases.

8.0 Conclusions

The results of an investigation study of coal mine waste dump under rainwater infiltration and steady-state response during rainfall event simulation are discussed in this paper. The following key observation can be drawn from the result

(a) The FoS decreases as the duration of rainfall increases until a critical duration is reached indicates water can enter by infiltration through its surface or groundwater seepage, and

(b) An increase in the underlying piezometric condition can potentially reach the base of the coal mine waste dump and may cause an upward lift or thrust.

Any variations from standard mandates should be identified and the justification for the above variations are presented where appropriate. Hence, the changes in FoS must be confirmed to an acceptable level of certainty to acknowledge instability.

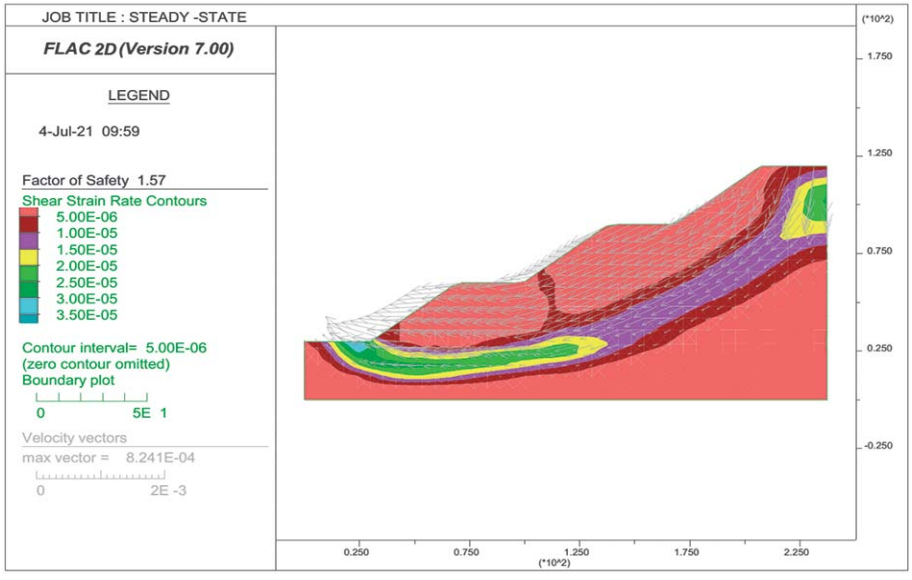

Fig.12: Model showing limiting surfaces and FoS

TABLE 9: PIEZOMETER WELL RECORD [WEST SIDE EXTERNAL DUMP]

Piezometric well no.	Location	Elevation (mRL)	Water (mRL)	Depth to Water (m)
PZB1	18°49'54.731"N, 79°29'11.085"E	837.25	708.50	1.50
PZB2	18°49'50.731"N, 79°29'06.202"E	836.65	708.66	1.34
PZB3	18°49'45.286"N, 79°29'06.811"E	836.39	708.92	1.08
PZB4	18°49'32.305"N, 79°28'50.154"E	836.21	709.50	0.50

TABLE 10: MATERIAL PROPERTIES UNDER UNDRAINED CONDITIONS IN FLAC^{2D}

Material property	Value
Wet Density, γ (kg/m^3)	2450
Internal angle of friction, ϕ(°)	20
Cohesion, c(kPa)	30
Elastic modulus (E), MPa	15-80
Poisson's ratio (υ)	0.2

Acknowledgements

The authors are very grateful to the Management and Officials, General Manager, Project Officer of SCCL, Srirampur opencast project for the field study. The authors also expresses their acknowledgement to the Department of Mining Engineering, National Institute of Technology, Raipur for allowing the paper to be published, and express their sincere gratitude to all those who help directly or indirectly in preparing the paper. The views expressed in the paper are individual to authors and are not necessary for the views of the Department of Mining Engineering, National Institute of Technology, Raipur, and Management of SCCL.

References

1. Bhattacharya, J. (2009): Guidance for Solving Environmental Challenges of Mining, Construction, Processing and Oil and Gas Fields Projects – Clearance, Design, Engineering, Inspection and Management, 1st Edition, Wide Publishing, India.
2. Blight, G. E. (2010): Geotechnical Engineering for Mine Waste Storage Facilities, CRC Press.
3. Briaud, J. L. (2013): Geotechnical Engineering: Unsaturated and Saturated Soils, John Wiley & Sons.
4. Chaulya, S. K., and Prasad, B. M. (2016): Sensing and Monitoring Technologies for Mines and Hazardous Areas - Monitoring and Prediction Technologies, Elsevier.
5. Collins, B. D., and Znidarcic, D. (2004): Stability Analyses of Rainfall-induced Landslides. *Journal of Geotechnical and Geoenvironmental Engineering*, ASCE, Vol. 130, Issue 4, pp 362-372.
6. Dash A K (2019): Analysis of accidents due to slope failure in Indian opencast coal mines. *Curr Sci* 117(2):304.
7. Desai, C. S., and Zaman, M. (2010): Advanced Geotechnical Engineering - Soil-Structure Interaction Using Computer and Material Models, CRC Press.
8. DGMS (Tech.) Circular No. 03/2020, Dhanbad, Dated-16.02.2020, Subject: Guidelines for Scientific Study under regulation 106 Coal Mines Regulations, 2017.
9. FLAC/Slope Users' Guide (2011): Command Reference, FISH and Theory and Background, Minneapolis Itasca Consulting Group
10. Hawley, M., and Cunning, J. (2017): Guidelines for Mine Waste Dump and Stockpile Design, CSIRO Publishing, CRC Press.
11. Horton, R. E. (1940): An Approach toward a Physical Interpretation of Infiltration Capacity, *Soil Science Society of American Journal*, Vol. 5, pp 399-417.
12. Hudak, P. F. (2005): Principles of Hydrogeology, 3rd Edition, CRC Press.
13. Kisch, M. (1959): The Theory of Seepage from Clay-blanketed Reservoirs, *Geotechnique*, Vol. 9, Issue 1, pp 9-21.
14. Koner, R., and Chakravarty, D. (2016): Numerical Analysis of Rainfall Effects in External Overburden Dump, *International Journal of Mining Science and Technology*, Volume 26, Issue 5, pp 825-831, Elsevier.
15. Kresic, N. (2007): Hydrogeology and Groundwater Modeling, 2nd Edition, CRC Press.
16. Nayak, P. K., Dash, A. K., and Dewangan, P. K., (2019): Design Considerations for Waste Dumps in Indian Opencast Coal Mines: A Critical Appraisal, ICOMS, 2nd International Conference, 13-14 December 2019, pp 19- 31.
17. Nayak, P. K., Dash, A. K., and Dewangan, P. K., (2021): Mine Waste Dump Instability and Monitoring Using Predictive Knowledge-Based Stability Rating and Hazard Classification System, ICOMS, 3rd International Conference, 22-23 Jan 2021, pp 195-204.
18. Naylor, D. J., and Pande, G. N. (1981): Finite Elements in Geotechnical Engineering, 1st Edition, Pineridge Press Ltd, Swansea, U.K.
19. Ng, C. W. W., and Shi, Q. (1998): Numerical Investigation of the Stability of Unsaturated Soil Slopes Subjected to Transient Seepage, *Computers and Geotechnics*, Vol.22, Issue 1, pp 1-28.
20. Novak, V., and Hlavacikova, H. (2019): Applied Soil Hydrology, Springer Nature.
21. Rahardjo, H., Ong, T. H., Rezaur, R. B., and Leong, E. C. (2007): Factors Controlling Instability of Homogeneous Soil Slopes under Rainfall, *Journal of Geotechnical and Geoenvironmental Engineering*, Vol 133, Issue 12, pp 1532-1543.
22. Rao, S. N. (2017): Hydrology – Problems with Solutions, PHI Learning.
23. Sen, Z. (2015): Practical and Applied Hydrogeology, ITU Hydraulics Lab. Maslak, 1st Edition, Elsevier.